MITSUBISHI ELECTRIC RESEARCH LABORATORIES
http://www.merl.com

Design and Optimization of Shallow-Angle Grating Coupler for Vertical Emission from Indium Phosphide Devices

Tang, Yingheng; Kojima, Keisuke; Gotoda, Mitsunobu; Nishikawa, Satoshi; Hayashi, Shusaku; Koike-Akino, Toshiaki; Parsons, Kieran; Meissner, Thomas; Song, Bowen; Sang, Fengqiao; Yi, Xiongsheng; Klamkin, Jonathan

TR2020-024 March 11, 2020

Abstract

We present the design and optimization strategy of shallow-angle grating couplers for vertical emission from InP devices, and then discuss the focusing effect of a 2D grating. Measured beam shape agrees well with the simulation results.

SPIE Photonics West

Design and Optimization of Shallow-Angle Grating Coupler for Vertical Emission from Indium Phosphide Devices

Yingheng Tang[a, b], Keisuke Kojima[a, c, *], Mitsunobu Gotoda[d], Satoshi Nishikawa[d], Shusaku Hayashi[d], Toshiaki Koike-Akino[a], Kieran Parsons[a], Thomas Meissner[c], Bowen Song[c], Fengqiao Sang[c], Xiongsheng Yi[c], and Jonathan Klamkin[c]

[a]Mitsubishi Electric Research Laboratories, 201 Broadway, Cambridge, MA 02139 USA
[b]Electrical and Computer Eng. Dept., Purdue University, West Lafeyette, IN 47907 USA
[c]Electrical and Computer Eng. Dept., University of California, Santa Barbara, CA 93106, USA
[d]Advanced Technology R&D Center, Mitsubishi Electric Corp., Amagasaki, Hyogo 661, Japan

ABSTRACT

We present the design and optimization strategy of shallow-angle grating couplers for vertical emission from InP devices, and then discuss the focusing effect of a 2D grating. Measured beam shape agrees well with the simulation results.

Keywords: hybrid integration, grating coupler, InP, silicon, PIC

1. INTRODUCTION

There have been many studies on integration of indium phosphide (InP) devices and silicon photonics.[1,2] Bonding of InP die onto a silicon on insulator wafer,[3] epitaxial growth of quantum dot lasers onto a silicon substrate,[4] and flip-chip bonding of an InP laser with an angle-etched mirror over a silicon grating[5] have been investigated. Grating out-couplers have also been extensively studied, however, a significant portion of the diffracted light is directed in an undesired direction, limiting the out-coupling efficiency.[6]
To address this limitation, Zhang et al.[7] demonstrated an inclined emitted laser with an emission angle of 55° using gratings within an InP-based laser cavity. An alternative approach is to fabricate buried gratings within a passive waveguide that could be external to a laser gain region. We recently proposed to use a bottom-emitting buried long-period grating such that the upward diffracted light is effectively reflected downward and the overall coupling efficiency is enhanced.[8] This concept can be implemented without precision lithography. The actual device design requires detailed simulations to understand the 2D beam properties in order to optimize the coupling efficiency into 2D silicon grating couplers. Also, experimental verification is required. In this work, we propose and design 2D gratings to shape the beam. 3D finite-difference time-domain (FDTD) numerical simulations are used to predict the emitted beam. Beam patterns of the prototyped grating couplers are measured; a nearly circular beam and a narrowing effect are demonstrated.

2. GRATING COUPLER INTEGRATION CONCEPT AND DESIGN

Figure 1 shows the conceptual side view of the shallow-angle grating coupler configuration, where InP and silicon waveguide gratings are used to couple the optical power from the InP waveguide to the silicon grating coupler. The cross-section of the InP device consists of an InP substrate, 0.35μm thick indium gallium arsenide phosphide (InGaAsP) layer (bandgap: 1.30 μm), a 0.15 μm deep etched grating, and a 0.47 μm thick InP upper cladding layer. The length of the InP grating section is 150 μm. To achieve a shallow diffraction angle (15° within InP and 55° in the air) and also to achieve a focusing effect onto a limited portion of the silicon waveguide grating, a long period grating (starting pitch: 10.59 μm) with linear chirp (pitch reduction: 0.1 μm per period) is employed. The output facet has an anti-reflection coating applied. With this 1D structure, a peak coupling efficiency in the

Further author information:
* E-mail: kojima@merl.com

range of $55-60\%$ is obtained by 2D FDTD simulations when the substrate thickness is between $40-120$ μm, where the device parameters are optimized for each substrate thickness. The 1-dB bandwidth is 60 nm and 40 nm for the substrate thickness of 40 μm and 120 μm, respectively.

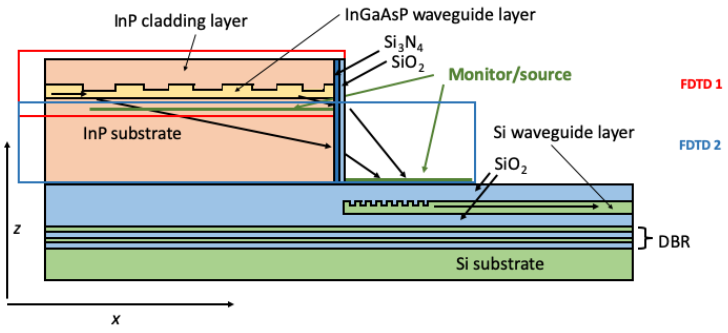

Figure 1. Schematic of the proposed grating coupler based integration scheme. Two-step 3D FDTD simulations were performed, where the electric field obtained in the first FDTD step is used for the source of the second step.

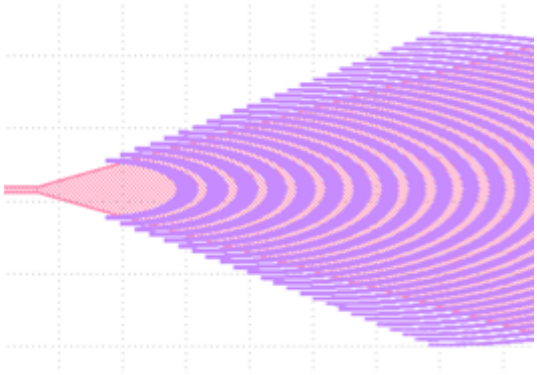

Figure 2. Mask pattern for the InP grating coupler, where purple patterns indicate the etched grating region, and orange patterns indicate the ridge region where the InP cladding layer is not etched away. The total ridge taper length is 200 μm.

3. 2D GRATING PRINCIPLE AND SIMULATIONS

For typical collimating silicon grating couplers, 2D grating lines are expressed as[9]

$$q\lambda = xn_s\ cos\phi_s - \ n_{eff}(x^2+y^2\ )^{1/2} \tag{1}$$

where q is an integer for each grating line, λ is the wavelength, x is the direction of propagation, y is the horizontal direction perpendicular to x, n is the refractive index of the InP substrate, θ is the emission angle into the InP substrate measured from the propagation direction, and n_{eff} is the effective refractive index of the waveguide. In order to create a focusing effect in the x and y directions, we add two ad hoc terms as follows:

$$q\lambda = xn_s\ cos\phi_s - \ n_{eff}(x^2+y^2\ )^{1/2} + \Delta_x x^2 + \Delta_x y^2 \tag{2}$$

where Δ_x and Δ_x are negative coefficients expressing the chirped grating in the x and y directions, respectively. Equation 2 can be solved numerically. The obtained curves are fitted to a series of ellipses. Note that the beam

is refracted at the vertical facet, so Δ_x and Δ_x need to be separately optimized. Figure 2 depicts the top view of the 2D InP grating coupler. The thickness of the etched region is first optimized in the center line ($y = 0$), and is made proportional to the distance from the grating center as y deviates from 0. The full width of the taper (fan shape) is 28°, and the total length of the grating taper is 200 μm. To simulate the beam propagation behavior out of the 2D grating, full 3D simulations are necessary. However, to fully simulate the entire grating coupler system, significant computing resources, in terms of memory, CPU cores, and computational time, are required. To circumvent this issue, we chose to split the 3D simulation into two regions as shown in Fig. 1. The first 3D FDTD simulation (FDTD 1) only involves the thin (thickness: 6 μm, length: 157 μm, width: 60 μm) region surrounding the InP grating, allowing finer mesh around the grating. A monitor below the grating receives the electromagnetic field, and is used as the source for the second simulation. The second 3D FDTD simulation (FDTD 2) includes a larger volume (thickness: 39 μm, length: 170 μm, width: 60 μm). However, with the exception of the facet area, the propagation is through the uniform region, so the mesh can be relatively coarse. We use the monitor placed just above the silicon grating to record the simulated final beam pattern for the discussion presented in the next section.

4. DEVICE FABRICATION AND EXPERIMENTAL RESULTS

The InP structure was grown using metalorganic chemical vapor deposition (MOCVD) and the composition and thickness of the InGaAsP waveguide were precisely controlled. Gratings are formed with electron beam lithography and reactive ion etching, to an etch depth of 0.15 μm. A 0.47μm thick InP cladding layer was regrown over the grating, also by MOCVD. Then the InP cladding layer was etched to form ridges outside of the grating taper region. After thinning the substrate to approximately 120 μm, the devices are cleaved into bars, and the facets are anti-reflection (AR) coated. The top view of the fabricated InP grating coupler prior to cleaving is shown in Fig. 3.

An external cavity tunable laser (wavelength: 1550 nm) and a lensed single mode fiber were used to couple light

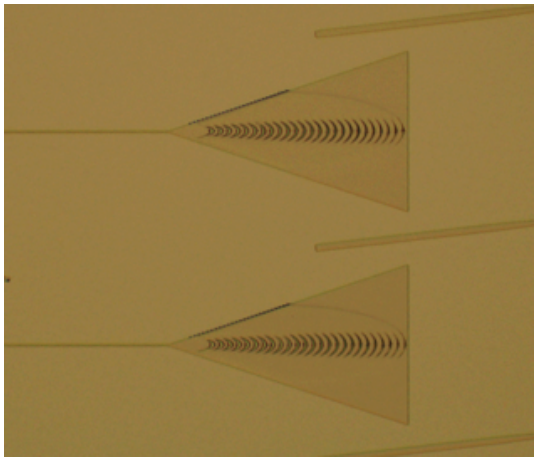

Figure 3. Top view microscope image of the fabricated InP grating coupler.

into the InP device. The polarization was controlled to be TE. For the measurement of the beam, we used an infra-red (IR) camera. The IR camera is arranged such that it looks into the coupler facet from 57° below the grating plane. By moving the camera, the beam shape is recorded at each distance. The beam is characterized by the full width at 50% or 13.5% ($1/e^2$) of the peak power. Figure 4 (a) shows the simulated beam pattern projected on a horizontal plane at 40 μm. The majority of the power is contained in the nearly-circular main lobe. There are weaker side lobes. Figure 4 (b) shows the measured beam pattern measured at the distance of 50 μm from the facet, and is projected using a computer software on the plane equivalent to the simulated case. (The distance of 50 μm from the facet corresponds to the beam shape on the silicon grating when the InP substrate thickness is 40 μm. The measured beam also has a nearly circular main lobe, and weaker side

lobes where the simulation predicted. Therefore, we confirmed a good agreement between the simulated and measured beam patterns. Figure 5 shows the full beam width in y direction as a function of the distance from the facet of three grating couplers with different chirp parameters Δ_y. As the absolute value of the chirp parameter increases, the beam is shown to be the narrowest, showing the effect of beam narrowing. For the full beam width at 13.5% of the peak power, the simulated values are 17.4 μm, 16.5 μm, and 15.4 μm for $\Delta_y = -0.6 \times 10^2/\mu$m, $-1.2 \times 10^2/\mu$m, and $-1.8 \times 10^2/\mu$m respectively. The measured values are, 20.4 μm, 20.2 μm, and 19.0 μm for the corresponding Δ_y values, respectively. So they are in good agreement in the expected beam shaping effect that the beam narrows more with increasing the chirping strength in the y direction.

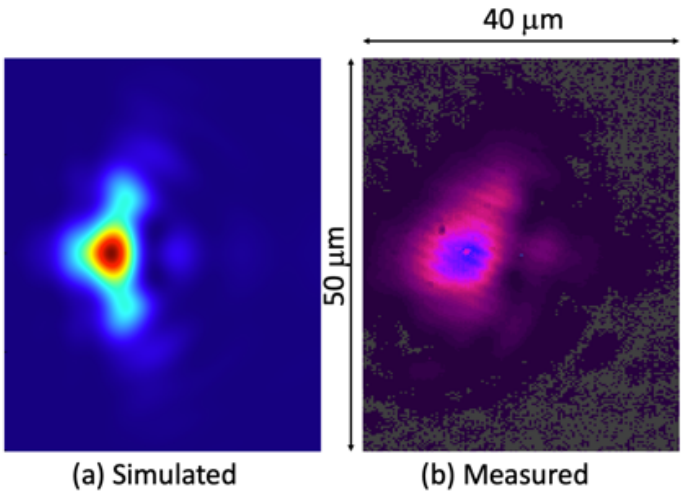

Figure 4. (a) Simulated and (b) measured beam pattern projected on a plane 40 μm below the InP grating plane. The grating chirp parameters are $\Delta_x = -1.6 \times 10^2/\mu$m, and $\Delta_y = -1.2 \times 10^2/\mu$m,.

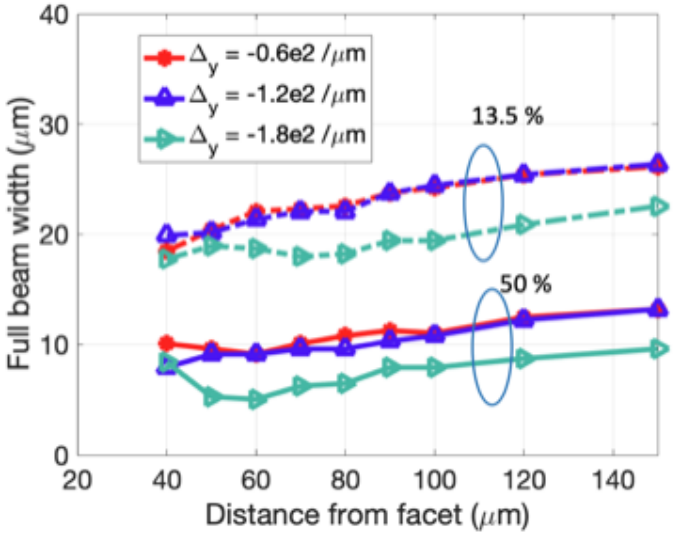

Figure 5. (Full beam width in the y direction (13.5% and 50% of the peak power) as a function of distance from facet. Δ_y is the grating chirp parameter in the y direction.

5. CONCLUSION

In this paper, we showed how to incorporate the 2D chirping effect in designing 2D gratings for shaping the beam from an shallow-angle InP grating coupler. We prototyped InP grating couplers, and the measured beam shape of the main lobe is nearly circular. The lateral beam narrowing is confirmed and agrees well with the simulation results.

REFERENCES

[1] Komljenovic, T., Davenport, M., Hulme, J., Liu, A. Y., Santis, C. T., Spott, A., Srinivasan, S., Stanton, E. J., Zhang, C., and Bowers, J. E., "Heterogeneous silicon photonic integrated circuits," *Journal of Lightwave Technology* **34**(1), 20–35 (2016).

[2] Bowers, J. E., "Heterogeneous photonic integration on silicon," in [*2018 European Conference on Optical Communication (ECOC)*], 1–3, IEEE (2018).

[3] Keyvaninia, S., Roelkens, G., Van Thourhout, D., Jany, C., Lamponi, M., Le Liepvre, A., Lelarge, F., Make, D., Duan, G.-H., Bordel, D., et al., "Demonstration of a heterogeneously integrated III-V/SOI single wavelength tunable laser," *Optics express* **21**(3), 3784–3792 (2013).

[4] Norman, J., Kennedy, M., Selvidge, J., Li, Q., Wan, Y., Liu, A. Y., Callahan, P. G., Echlin, M. P., Pollock, T. M., Lau, K. M., et al., "Electrically pumped continuous wave quantum dot lasers epitaxially grown on patterned, on-axis (001) si," *Optics Express* **25**(4), 3927–3934 (2017).

[5] Song, B., Stagarescu, C., Ristic, S., Behfar, A., and Klamkin, J., "3D integrated hybrid silicon laser," *Optics Express* **24**(10), 10435–10444 (2016).

[6] Kojima, K., Kameya, M., Noda, S., and Kyuma, K., "High efficiency surface-emitting distributed bragg reflector laser array," *Electronics Letters* **24**(5), 283–284 (1988).

[7] Zhang, Y., Su, Y., Bi, Y., Pan, J., Yu, H., Zhang, Y., Sun, J., Sun, X., and Chong, M., "Inclined emitting slotted single-mode laser with 1.7 ° vertical divergence angle for pic applications," *Optics Letters* **43**(1), 86–89 (2018).

[8] Kojima, K., Koike-Akino, T., Tahersima, M., Parsons, K., Meissner, T., Song, B., and Klamkin, J., "Shallow-angle grating coupler for vertical emission from indium phosphide devices," in [*Integrated Photonics Research, Silicon and Nanophotonics*], IM3A–6, Optical Society of America (2019).

[9] Waldhäusl, R., Schnabel, B., Dannberg, P., Kley, E.-B., Bräuer, A., and Karthe, W., "Efficient coupling into polymer waveguides by gratings," *Applied Optics* **36**(36), 9383–9390 (1997).